Available online at www.sciencedirect.com
SCIENCE DIRECT®
Journal of Catalysis 226 (2004) 111–119
JOURNAL OF CATALYSIS
www.elsevier.com/locate/jcat

A mononuclear gold complex catalyst supported on MgO: spectroscopic characterization during ethylene hydrogenation catalysis

Javier Guzman, Bruce C. Gates *

Department of Chemical Engineering and Materials Science, University of California, Davis, CA 95616, USA

Received 12 December 2003; revised 29 April 2004; accepted 6 May 2004

Available online 15 June 2004

Abstract

Mononuclear gold complexes supported on MgO powder were prepared by adsorption of $Au(CH_3)_2(C_5H_7O_2)$ and tested as catalysts for ethylene hydrogenation at atmospheric pressure and 353 K. The catalyst was characterized in the working state with extended X-ray absorption fine structure (EXAFS), X-ray absorption near-edge structure (XANES), and infrared (IR) spectroscopies. EXAFS and XANES data demonstrate the presence of mononuclear Au(III) complexes as the predominant surface gold species during catalysis, with no evidence of metallic gold clusters, confirmed by the lack of Au–Au contributions in the EXAFS spectra and the presence of the characteristic features of Au(III) in the XANES spectra. The mononuclear gold complex is bonded to two oxygen atoms of the MgO surface at an Au–O distance of 2.16 Å. Ethyl and π-bonded ethylene on the mononuclear gold were identified by IR spectroscopy, with the former identified as a reactive intermediate and the latter apparently a spectator or involved as an intermediate in virtually equilibrated steps. Hydrogen on the mononuclear gold is inferred to form by dissociative adsorption of H_2, as indicated by the order of the catalytic reaction in H_2 of 0.5.

Keywords: Gold; Ethylene; Hydrogenation; Ethyl; Mononuclear gold complex; EXAFS; XANES; IR

1. Introduction

Ethylene hydrogenation is a widely used test reaction for supported metal particles and surfaces, offering the advantages of small reactant molecules that form adsorbates (ligands) that may be identified by infrared (IR) [1] or sum frequency generation (SFG) spectroscopy [2] under reaction conditions. With many metals, the reaction occurs under such mild conditions that significant alteration of the catalyst structure, such as sintering of the metal [3], can be avoided. Spectra of supported mononuclear metal complex catalysts for ethylene hydrogenation allow characterization of the ligands on the metal, providing a basis for comparison of metal surfaces and cationic metal complexes (such as Wilkinson's catalyst) as catalysts [4].

Notwithstanding the novelty and practical importance of supported single-site metal complex catalysts (exemplified by the commercial successes of metallocenes for alkene polymerization [5]), they are much less well understood than transition-metal complexes in solution. Spectra characterizing precisely synthesized catalysts of this type promise rapid advances in the understanding of how they function [6].

Our goal was to investigate the performance of a site-isolated mononuclear gold complex catalyst and to identify the reactant-derived ligands on the metal during ethylene hydrogenation catalysis and to characterize the metal–support bonding. We report rates of catalytic hydrogenation of ethylene and extended X-ray absorption fine structure (EXAFS), X-ray absorption near-edge structure (XANES), and IR spectra of a MgO-supported gold complex catalyst in the working state. Gold was chosen because mononuclear gold complexes are used frequently in organometallic chemistry, having been identified as catalysts for reactions including addition of alcohols to alkynes [7], asymmetric aldol reactions [8], C–C bond formation [9], oxidative carbonylation of amines [10], selective hydrosilylation of aldehydes [11], addition of water or methanol to terminal alkynes [12], formation of hydrogen peroxide [13], selective oxidation of glycerol to glyceric acid [14], hydrogenation of crotonaldehyde and of butenal [15], and hydrochlorination of acetylene [16]. We recently communicated evidence of a

* Corresponding author.
E-mail address: bcgates@ucdavis.edu (B.C. Gates).

0021-9517/$ – see front matter
doi:10.1016/j.jcat.2004.05.014

MgO-supported mononuclear gold complex as an ethylene hydrogenation catalyst [17]; here, we provide a full report of the catalyst performance and characterization.

2. Experimental methods

2.1. Materials, sample preparation, and handling

The synthesis and handling of the MgO-supported mononuclear gold complex were carried out as before [17] under anaerobic and anhydrous conditions on a double-manifold Schlenk vacuum line and in a glove box purged with N_2 that was recirculated through traps containing particles of supported Cu and zeolite 4A for removal of O_2 and moisture, respectively. He (Matheson, 99.999%) and ethylene (Matheson, 99.5%) were purified by passage through similar traps. H_2 was supplied by Matheson (99.999%) or generated by electrolysis of water in a Balston generator (99.99%) and purified by passage through traps. The MgO support (EM Science, 97%) was calcined in O_2 at 673 K for 2 h (BET surface area, 60 $m^2\,g^{-1}$), isolated, and stored in a glove box until it was used. *n*-Pentane solvent (Fisher, 99%) was dried and purified by refluxing over sodium benzophenone ketyl and deoxygenated by sparging of N_2. The precursor $Au(CH_3)_2(acac)$ (Strem, 98%; acac is $C_5H_7O_2$) was purified by sublimation after it was received; this compound is temperature sensitive and requires refrigeration.

The samples were prepared by slurrying $Au(CH_3)_2(acac)$ in dried and deoxygenated *n*-pentane with partially dehydroxylated MgO powder. The slurry was stirred for 1 day and the solvent removed by evacuation (pressure $< 10^{-3}$ Torr) for 1 day.

2.2. Ethylene hydrogenation catalysis in a plug–flow reactor

Ethylene hydrogenation catalysis was carried out in a once-through tubular quartz reactor (8 mm i.d.) at atmospheric pressure and 353 K. The reactor in the glove box was loaded with a mixture of inert α-Al_2O_3 and catalyst powder (typically 100–200 mg) in a 100:1 ratio by mass. The loaded reactor was isolated, removed from the glove box, and installed in a flow system without contact of the catalyst with air or moisture.

An on-line gas chromatograph (Hewlett–Packard, HP-5890 Series II), equipped with a 30-m × 0.53-mm DB-624 (J&W Scientific) capillary column (with N_2 as the carrier gas, flowing at 2.5 mL (NTP) min^{-1}) and a flame-ionization detector, was used to analyze the reaction products. Conversions of ethylene to ethane at steady state were differential (less than 5%), determining reaction rates directly.

The total feed flow rate ($He + H_2 + C_2H_4$) to the reactor was 100 mL (NTP) min^{-1}. Under these conditions, the reactor is well approximated as an isothermal plug–flow reactor. Catalytic hydrogenation of ethylene was typically carried out with an ethylene partial pressure ($P_{ethylene}$) of 40 Torr and a $P_{hydrogen}$ of 160 Torr at 353 ± 2 K. Kinetics experiments were done by varying the ethylene and H_2 partial pressures in the range 35–300 and 35–450 Torr, respectively. Experiments were also carried out at other reaction temperatures. Steady-state reaction rates, reported as turnover frequency (TOF, rate of reaction per Au atom per second), were determined from differential conversions with an accuracy of about ±10%.

2.3. X-ray absorption spectra of functioning catalysts

X-ray absorption experiments were performed at beamline X-11A of the National Synchrotron Light Source (NSLS) at Brookhaven National Laboratory, Upton, NY. The ring current was 110–250 mA, and the storage ring operated with an electron energy of 2.5 GeV. Higher harmonics in the X-ray beam were minimized by detuning the Si(111) double crystal monochromator by 20–25% at the Au L_{III} edge (11919 eV).

Transmission X-ray absorption spectroscopy (XAS) experiments were used to characterize the sample in the presence of flowing mixtures of He, H_2, and C_2H_4 as hydrogenation catalysis took place; the conditions essentially matched those of the flow reactor experiments described in the preceding section. In a N_2-filled glove box at the synchrotron, 0.2 g of powder sample was loaded into an XAS cell/reactor (the powder catalyst was held in the middle of an XAS cell/reactor by glass wool plugs), which was then isolated, removed from the glove box, and installed in the flow system at the beamline without contact of the catalyst with air or moisture. The XAS cell/reactor operating at low conversions is well approximated as an isothermal plug-flow reactor; details of its design and analysis of its operation are presented elsewhere [18].

2.4. IR spectroscopy of functioning catalysts

Catalysis was also carried out in an IR cell/reactor (In-situ Research Institute, Inc., South Bend, IN) under conditions similar to those used in the kinetics and X-ray absorption spectroscopy experiments. A Bruker IFS 66v spectrometer with a spectral resolution of 4 cm^{-1} was used to collect transmission IR spectra of the sample powder. Samples were pressed into self-supporting wafers and loaded into the cell connected to a vacuum/adsorption system, which allowed recording of spectra while the treatment gases flowed through and around the wafer during catalysis. IR spectra of adsorbate ligands were determined by subtracting the spectrum of the sample in He from that of the sample in the treatment gas. Spectra characterizing the ligands present during steady-state ethylene hydrogenation catalysis were recorded under various reaction conditions. Each reported spectrum is the average of 128–512 scans.

Table 1
Crystallographic data characterizing the reference compounds and Fourier transform ranges used in the EXAFS analysis[a]

Reference compound	Shell	Crystallographic data			Fourier transform		
		N	R (Å)	Ref.	Δk (Å^{-1})	Δr (Å)	n[b]
Au	Au–Au	12	2.88	[22]	1.00–20.00	0.00–8.00	3
Au foil	Au–Au	12	2.88	[21]	2.64–19.60	1.50–3.40	3
$Au(CH_3)_2(acac)$	Au–O	2	2.08	[21]	2.61–16.31	1.30–2.40	2
$Na_2Pt(OH)_6$	Pt–O (Au–O)	6	2.05	[20]	2.67–15.69	0.00–2.10	2
$Au(CH_3)_2(acac)$	Au–C	2	2.05	[21]	2.64–19.60	1.50–3.40	2
$AuMg_3$	Au–Mg	8	2.70	[23]	0.00–20.00	0.00–8.00	3

[a] Notation: N is the coordination number, R the distance between absorber and backscatterer atoms, k the wave vector, and Δk and Δr the range intervals used in the Fourier transformation.
[b] A k^n weighting was used in the Fourier transformation of the data for purposes of extracting the reference phase and amplitude functions of the absorber–backscatterer pair.

3. EXAFS data analysis

Analysis of the EXAFS data was carried out with a difference file technique by use of the software XDAP [19]. No attempt was made to account for the small atomic X-ray absorption fine structure (data obtained at low values of r, the distance from the absorber atom, Au) of the spectrum other than by application of standard background subtraction techniques. Iterative fitting was carried out until excellent agreement was attained between the calculated k^0-, k^1-, and k^2-weighted data (k is the photoelectron wave vector) and the postulated model. Experimentally determined reference files prepared from EXAFS data representing materials of known structure [20,21] and theoretically determined reference files calculated by using the software FEFF 7.0 or FEFF 8.0 [22,23] were used in the analysis (Table 1). Details of the preparation of the reference files and data analysis procedures are presented elsewhere [24,25]. The number of parameters used in fitting the data to each model is justified statistically by the Nyquist theorem. The fitting ranges in both momentum space and real space were determined by the data quality. The quality of the fitting was confirmed by the values of fit diagnostic parameters, ε_ν^2 (goodness of fit) and the variances between the data and the model predictions for the EXAFS function χ and the Fourier transform of χ (for k^0-, k^1-, and k^2-weighting of the data).

4. Results

4.1. Synthesis of mononuclear Au(III) complexes supported on MgO

Adsorption of $Au^{III}(CH_3)_2(acac)$ on MgO that had been calcined at 673 K led to the formation of supported $Au^{III}(CH_3)_2\{OMg\}_2$ (where the {OMg} ligands are part of the support), consistent with our previous report [17] and evidenced by the IR bands in the ν_{CH} region at 2954 and 2910 cm^{-1} (which nearly match those representing the CH_3 groups in solid $Au(CH_3)_2(acac)$) and by the lack of Au–Au first- and second-shell contributions in the EXAFS spectrum (Fig. 1). No Au–Au contributions were found at distances typical of Au–Au bonds (e.g., 2.88 Å), consistent with the inference that the supported species were highly dispersed and mononuclear. The EXAFS data show that the gold atom in the surface complex was bonded to two oxygen atoms (Table 2). These are inferred to be part of the MgO surface, because the Au–O distance was found to be 2.16 Å (vs 2.08 Å in $Au(CH_3)_2(acac)$ [26]), typical of M–O bonding distances in other zeolite- and oxide-supported mononuclear group 8 metal complexes [27].

Table 2
EXAFS results characterizing MgO-supported mononuclear gold complexes[a]

Shell	N	R (Å)	$\Delta\sigma^2 \times 10^3$ (Å^2)	ΔE_0 (eV)
Au–Au	–[b]	–	–	–
Au–O_s	2.1	2.16	0.20	3.45
Au–O_l	0.9	2.85	1.04	1.02
Au–Mg	0.9	2.72	1.45	1.35
Au–C	2.0	2.04	2.35	2.57

[a] Notation: N, coordination number; R, distance between absorber and backscatterer atoms; $\Delta\sigma^2$, Debye–Waller factor; ΔE_0, inner potential correction. Expected errors N: ±10%, R: ±0.02 Å, $\Delta\sigma^2$: ±20%, ΔE_0: ±20%. The subscripts s and l refer to short and long, respectively.
[b] Undetectable.

The XANES data characterizing this supported gold complex are virtually identical to those characterizing crystalline $Au(CH_3)_2(acac)$ [28]. This comparison indicates that the gold retained its oxidation state of +III after chemisorption of the precursor. This point is addressed further below on the basis of XANES data characterizing the working catalyst.

4.2. Kinetics of ethylene hydrogenation

The catalytic activities are reported per total Au atom, and the EXAFS data, summarized below, show that they were all present in mononuclear complexes in the working catalysts.

After a brief transient induction period (typically, 30 min) [29], the supported gold complex catalyst was found to have stable activity for ethylene hydrogenation at 353 K, $P_{hydrogen} = 160$ Torr, $P_{ethylene} = 40$ Torr, and $P_{He} = 560$ Torr, corresponding to a reaction rate (determined from differential conversion data) of 2.9×10^{-3} molecules of

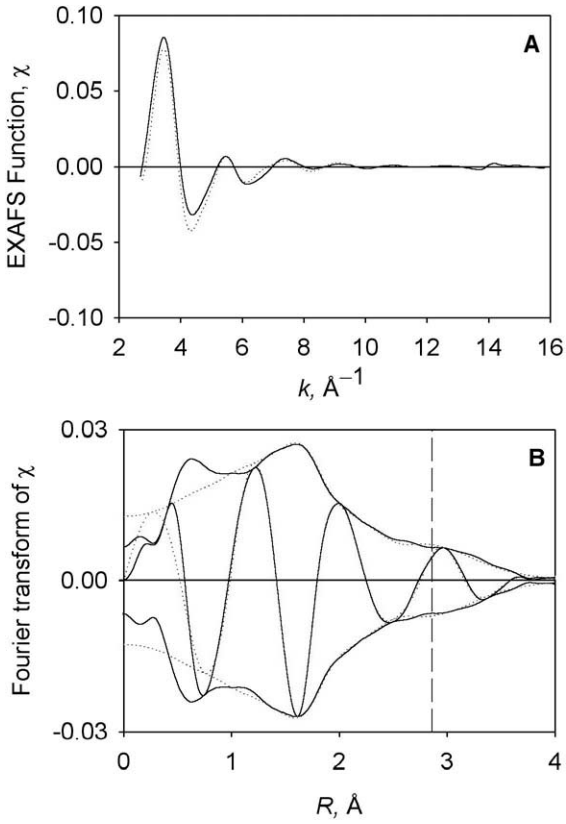

Fig. 1. Results of EXAFS analysis characterizing MgO-supported mononuclear gold complexes: (A) Experimental EXAFS function (solid line) and sum of the calculated Au–Au + Au–O_s + Au–O_l + Au–Mg + Au–C contributions (dotted line). (B) Imaginary part and magnitude of uncorrected Fourier transform (k^0 weighted) of experimental EXAFS function (solid line) and sum of the calculated Au–Au + Au–O_s + Au–O_l + Au–Mg + Au–C contributions (dotted line). The Au–Au bonding distance (2.88 Å) in bulk gold metal is shown by a vertical dashed line.

ethylene converted (Au atom × s)$^{-1}$. The only product observed was ethane, and there was no measurable conversion of ethylene and H_2 in the absence of catalyst. The support alone had a negligible activity.

Kinetics data were collected for ethylene hydrogenation catalyzed by the supported gold complexes. The apparent activation energy determined from the dependence of TOF on temperature was found to be 51 kJ mol^{-1} (Fig. 2). Data characterizing steady-state ethylene hydrogenation at 353 K indicate that the reaction order in H_2 (at $P_{\text{ethylene}} = 40$ Torr) was 0.5 and that the reaction order in ethylene (at $P_{\text{hydrogen}} =$ 160 Torr) was 0.0 (Fig. 3).

4.3. XANES evidence of oxidation state of gold during ethylene hydrogenation catalysis

XANES data provide information about the electron density (oxidation state) and site symmetries of the gold species. XANES peak locations and intensities characterizing reference materials containing gold in various oxidation states, summarized elsewhere [29–31], provide a basis for interpretation of the data. The XANES spectra characterizing com-

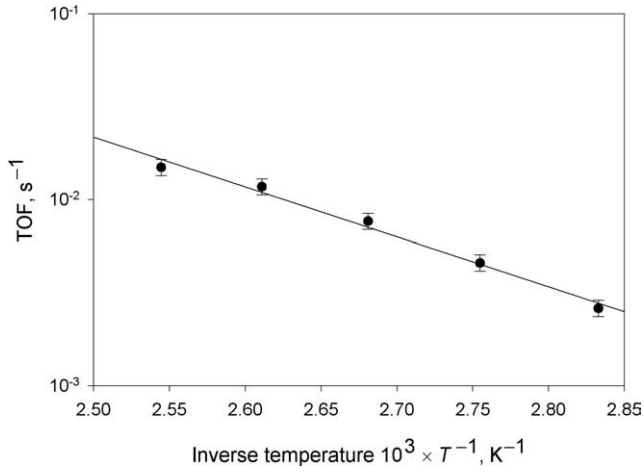

Fig. 2. Arrhenius plot for ethylene hydrogenation catalyzed by mononuclear gold complexes supported on MgO. Reaction conditions: 160 Torr of H_2, 40 Torr of C_2H_4, 560 Torr of He. The total feed flow rate was 100 mL (NTP) min^{-1}, and the mass of catalyst was 0.10 g.

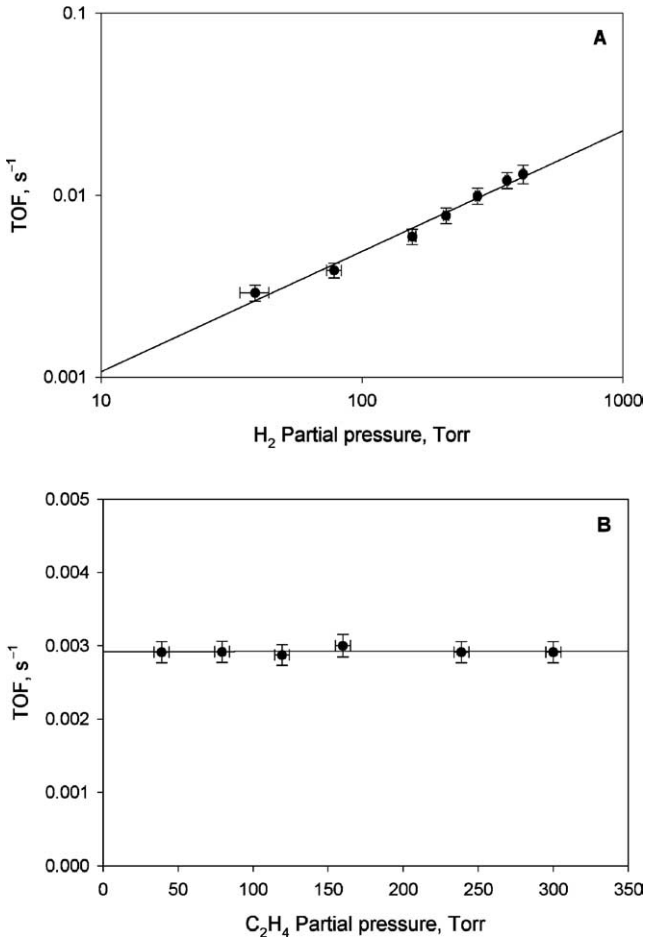

Fig. 3. Kinetics of ethylene hydrogenation catalyzed by MgO-supported mononuclear gold complexes at 353 K. (A) Dependence of rate on H_2 partial pressure at a constant ethylene partial pressure of 40 Torr (the reaction order in H_2 is 0.5). (B) Dependence of rate on ethylene partial pressure at a constant H_2 partial pressure of 280 Torr (the reaction order in ethylene is 0.0).

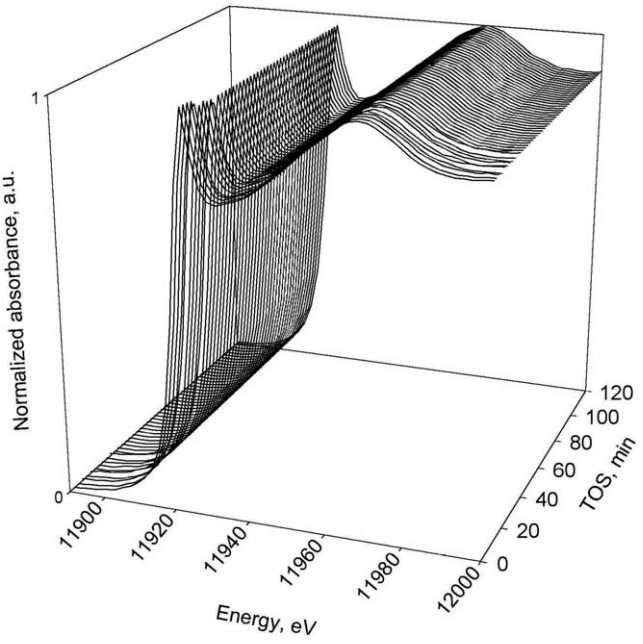

Fig. 4. XANES data characterizing MgO-supported mononuclear gold complexes during ethylene hydrogenation catalysis at atmospheric pressure and 353 K. Conditions: 353 K, 760 Torr (40–460 Torr of H_2, 40–220 Torr of C_2H_4, and the balance He); the total feed flow rate was 100 mL (NTP) min^{-1}; the mass of catalyst was 0.1 g.

plexes containing Au(III) show a prominent feature (white line) centered at an energy 4 eV higher than that of the Au L_{III} edge. This absorption peak is missing from the spectra of metallic gold because of the complete occupancy of the *d* states (the gold ground-state electron configuration is $[Xe]4f^{14}5d^{10}6s^1$). Furthermore, the spectrum of Au(III) shows a broad shoulder at an energy 50 eV higher than that of the X-ray absorption edge, whereas the spectrum of Au(0) shows a shoulder at 15 eV and intense peaks at 25 and 50 eV beyond the edge [29–31].

The XANES data characterizing MgO-supported gold complexes during catalysis at 353 K and at 760 Torr (160 Torr of H_2, 40 Torr of C_2H_4, and the balance He) show that the gold maintained the oxidation state of +III, as shown by the retention of the intense peak at an energy 4 eV higher than that of the X-ray absorption edge and the broad shoulder at 50 eV beyond the X-ray absorption edge (Fig. 4). Similar results (not shown) were obtained when the ethylene and H_2 partial pressures were varied in catalysis experiments; Au(III) complexes were identified in all cases during catalysis; the spectra were indistinguishable from that of Fig. 4.

The only observed changes in the XANES data characterizing MgO-supported gold complexes during catalysis occurred within the first 30 min on stream (when the catalyst was approaching steady state), consisting of a slight reduction in intensity of the white line (Fig. 4), which is attributed to changes in site symmetry of the mononuclear gold species rather than changes in oxidation state of gold.

Table 3
EXAFS results characterizing MgO-supported mononuclear gold complexes during ethylene hydrogenation catalysis at atmospheric pressure and 353 K[a]

Conditions during scan			Shell	*N*	*R* (Å)	$\Delta\sigma^2$ $\times 10^3$ (Å^2)	ΔE_0 (eV)
$P_{ethylene}$ (Torr)	$P_{hydrogen}$ (Torr)	P_{helium} (Torr)					
40	40	680	Au–Au	–[b]	–	–	–
			$Au–O_s$	2.0	2.18	1.34	2.78
			$Au–O_l$	0.8	2.87	2.53	3.12
			Au–Mg	0.8	2.74	2.56	2.66
			Au–C	–[b]	–	–	–
40	160	560	Au–Au	–[b]	–	–	–
			$Au–O_s$	2.0	2.18	2.14	2.34
			$Au–O_l$	0.9	2.87	3.13	4.64
			Au–Mg	0.9	2.73	2.46	3.17
			Au–C	–[b]	–	–	–
220	220	320	Au–Au	–[b]	–	–	–
			$Au–O_s$	2.0	2.19	3.24	1.78
			$Au–O_l$	0.9	2.88	3.22	8.56
			Au–Mg	0.9	2.74	2.46	5.32
			Au–C	0.6	1.99	−1.23	6.23
220	460	80	Au–Au	–[b]	–	–	–
			$Au–O_s$	2.0	2.19	2.26	3.51
			$Au–O_l$	0.9	2.88	2.46	5.89
			Au–Mg	0.9	2.74	3.75	4.36
			Au–C	0.5	1.94	−1.17	5.13

[a] Notation: *N*, coordination number; *R*, distance between absorber and backscatterer atoms; $\Delta\sigma^2$, Debye–Waller factor; ΔE_0, inner potential correction. The total feed flow rate was 100 mL (NTP) min^{-1}. Expected errors N: ± 10%, R: ± 0.02 Å, $\Delta\sigma^2$: ± 20%, ΔE_0: ± 20%. The subscripts s and l refer to short and long, respectively.

[b] Undetectable.

4.4. EXAFS evidence of structure of gold complex during ethylene hydrogenation catalysis

The EXAFS parameters characterizing the working catalyst at 353 K and 760 Torr ($P_{ethylene}$ in the range of 40–220 Torr, $P_{hydrogen}$ in the range of 40–460 Torr, and the balance He) show that the mononuclear gold complexes were maintained, as shown by the lack of Au–Au first- and higher-shell contributions in the EXAFS spectrum (Table 3). This result and the observation that the support was catalytically inactive for ethylene hydrogenation bolster the inference that mononuclear gold complexes were the catalytically active species.

A small contribution in the EXAFS spectrum attributed to Au–C (Table 3) is not sufficient to distinguish among possible reaction intermediates bonded to the gold; however, this contribution is consistent with the presence of hydrocarbon ligands (possibly reaction intermediates) on the gold.

Although the nuclearity of the gold complexes was maintained during catalysis, the structural parameters determined by EXAFS spectroscopy that characterize the metal complex–support interaction were altered when the catalyst was brought in contact with the reactants, as indicated by changes in the $Au–O_s$ and $Au–O_l$ contributions (the sub-

Table 4
Infrared bands characterizing adsorbates on mononuclear gold complexes supported on MgO during ethylene hydrogenation catalysis[a] and vibrational spectra of reference materials[b]

Sample	Band locations (cm^{-1})	Adsorbate	Reference
Au/MgO	2960, 2923, 2865	ethyl	[This work]
Ir_4/γ-Al_2O_3	2957, 2929, 2863	ethyl	[32]
CH_3CH_2Cl	2967, 2947, 2881	ethyl	[39]
Pt(111)	2918	ethyl	[40]
Au/MgO	3085	π-bonded ethylene	[This work]
Ir_6/MgO	3090	π-bonded ethylene	[33]
Ir_4/γ-Al_2O_3	3060, 3026	π-bonded ethylene	[32]
Pt(111)	3060	π-bonded ethylene	[35]

[a] Conditions of ethylene hydrogenation catalysis: 353 K, 760 Torr (40–400 Torr of H_2, 40 Torr of C_2H_4, and the balance He), and the total feed flow rate was 100 mL (NTP) min^{-1}.

[b] Data obtained at relatively low ethylene partial pressures, which are comparable with our catalytic conditions.

scripts s and l refer to short and long, respectively) and a weak contribution tentatively identified as Au–Mg (Tables 2 and 3). The data are consistent with inferences [3,32] that the presence of ligands on supported metal complexes or clusters during alkene hydrogenation catalysis alters the structural parameters characterizing the metal–support interface.

4.5. IR evidence of adsorbates on mononuclear gold complex during ethylene hydrogenation catalysis

IR spectra of the ligands present on the mononuclear gold complexes during pretreatment of the catalyst in flowing ethylene or H_2 and also during steady-state ethylene hydrogenation catalysis were collected over a wide range of conditions so that the different adsorbates could be identified and their band intensities correlated with catalytic activity. When H_2, ethylene, or a catalytically reacting mixture of H_2, ethylene, and He was brought in contact with the MgO support without gold, no ethylene-derived ligands were observed.

The IR spectra show that ethylene (at partial pressures of 40–760 Torr, in He, and at 300 or 353 K) interacts with the mononuclear gold complexes to form only the adsorbed species characterized by the band at 3085 cm^{-1}, which is assigned to π-bonded ethylene on mononuclear gold (π-C_2H_4/Au{OMg}$_2$, Table 4), nearly matching the spectra attributed to π-bonded ethylene on Ir_4/γ-Al_2O_3 (3060 cm^{-1}) [32], Ir_6/MgO (3090 cm^{-1}) [33], and Rh(111) [34] or Pt(111) (3060 cm^{-1}) [35].[1]

[1] The CH_2 stretch of π-bonded ethylene was observed at a frequency 25 cm^{-1} higher than that of π-bonded ethylene on Rh(111) [34] or Pt(111) [35]. However, this band has been observed at a similar frequency for π-bonded ethylene on supported iridium clusters (Ir_6/MgO), and it has been suggested [33] that the difference in frequency indicates that π-bonded ethylene on Ir_6/MgO is considerably less hybridized than that on the single crystals. Thus, we infer that a similar effect may pertain to π-bonded ethylene in the mononuclear gold complexes.

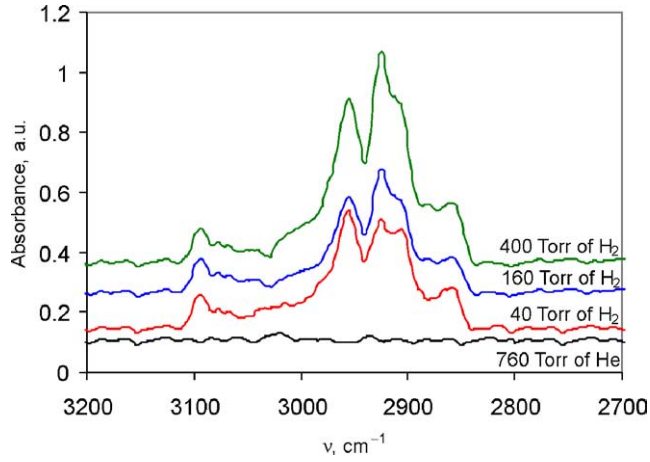

Fig. 5. IR spectra characterizing the C–H-stretching frequency range of the ligands on mononuclear gold complexes during ethylene hydrogenation catalysis at 353 K, 760 Torr (40–400 Torr of H_2, 40 Torr of C_2H_4, and the balance He), and at a total feed flow rate of 100 mL (NTP) min^{-1}; the mass of catalyst was 0.02 g.

The IR spectra are not sensitive enough to determine whether gold hydride formed when H_2 was brought in contact with the mononuclear gold complex at 100–760 Torr and 300 K, but we do not rule out the possibility [36,37]. Furthermore, the IR spectra did not show any evidence of CH_3 ligands bonded to the gold, consistent with the EXAFS data (Table 3) indicating removal of methyl groups initially bonded to the gold complex.

When the gold complex was brought in contact with a mixture of ethylene, H_2, and He ($P_{ethylene}$ = 40 Torr, $P_{hydrogen}$ = 40–400 Torr, the balance He) at 353 K and 760 Torr, the IR spectra demonstrated the presence of ligands during catalysis (with values of TOF in the range of (0.2–2.2) $\times$ 10^{-2} molecules of ethylene converted (Au atom $\times$ s)$^{-1}$) indicated by the presence of bands in the C–H-stretching range at 3085, 2960, 2923, and 2865 cm^{-1} (Fig. 5). These results, and those showing that there were no measurable IR peaks of adsorbates in the presence of MgO alone, bolster the inference of the formation of ethylene-derived ligands on the gold and not on the support. The peak at 3085 cm^{-1} is assigned, as before, to π-bonded ethylene on gold (π-C_2H_4/Au{OMg}$_2$) (Table 4). The bands at 2960, 2923, and 2865 cm^{-1} are assigned to ethyl on gold (CH_3CH_2Au{OMg}$_2$) (Table 4), because they occur at frequencies similar to those of ethyl chloride (2967, 2947, and 2881 cm^{-1}) [38] and of ethyl on Ir_4/γ-Al_2O_3 (2957, 2929, and 2863 cm^{-1}) [32] and on Pt(111) (2918 cm^{-1}) [39]. Specifically, the peak at 2865 cm^{-1} occurs at a frequency similar to that of the CH_3 symmetric stretch of ethyl chloride (and 2881 cm^{-1}) [38]. Additional peaks representative of ethyl (CH_2 stretch and CH_3 antisymmetric stretch) were not discernible above the noise in the spectra.

5. Discussion

5.1. Identification of supported mononuclear gold complexes as catalytically active species

The EXAFS data show that the mononuclear Au(III) complexes on MgO were the only detected gold species during catalytic hydrogenation of ethylene. There was no evidence of metallic gold clusters or any other gold species during catalysis. Furthermore, because there was no measurable conversion of ethylene and H_2 in the absence of catalyst and the support alone was catalytically inactive for ethylene hydrogenation, we infer that the supported mononuclear gold complexes are the catalytically active species.

Additional evidence supporting this conclusion is provided by IR spectroscopy demonstrating the formation of ethylene-derived ligands on the gold centers when ethylene and H_2 came in contact with the supported gold complex; when ethylene and H_2 came in contact with the support alone, there was no detectable formation of ethylene-derived ligands.

5.2. Metal–support bonding and stability of the supported gold complex during ethylene hydrogenation catalysis

The XANES data characterizing the gold complex on MgO during catalysis show that the oxidation state of gold remained as +III, and the small change observed in the spectrum during the 30-min induction period is suggested to be evidence of the removal of CH_3 ligands from the precursor $Au^{III}(CH_3)_2\{OMg\}_2$ and the formation of other ligands on the gold. The IR results confirm the removal of the methyl groups during H_2 treatment and demonstrate the formation of ethylene-derived ligands during treatment in ethylene and H_2.

The EXAFS data characterizing the supported gold complex during catalysis at 353 K demonstrate the stability of the complex for more than 4 h TOS, as indicated by the lack of Au–Au first- and second-shell contributions. We infer that our reaction conditions were mild enough to prevent changes of the single-site metal complex, such as aggregation of gold.

Although the nuclearity of the gold complexes was maintained during catalysis, the EXAFS parameters characterizing the gold–support interaction (Au–oxygen and Au–Mg contributions) were altered slightly from those of the catalyst precursor. The results (Table 3) indicate a small increase in the Au–oxygen distance, but the difference between the two distances (0.03 Å) is barely larger than the estimated error (±0.02 Å). Thus, the data suggest but do not demonstrate that the interactions between the ligands and the gold affect the metal–support bonding. Such interactions are expected to be maximized for the smallest metal complexes or clusters [3,32]. Changes in the Au–oxygen distance might be related to changes in the degree of charge polarization of the metal at the metal–support interface (but other explanations are not excluded).

5.3. Comparison between mononuclear gold complexes and gold clusters as hydrogenation catalysts

Our results show that supported mononuclear gold complexes are catalytically active for ethylene hydrogenation. To test whether supported gold clusters might also be catalysts for this reaction, we also investigated a family of supported samples containing gold clusters of various sizes (made by adsorption of $Au(CH_3)_2(acac)$ on MgO, followed by treatment in flowing He at various temperatures to cause autoreduction and sintering). The results, already communicated [17], indicate that the ethylene hydrogenation activity decreased as the Au–Au coordination number (and the average gold cluster size [40])[2] in the catalysts prior to use increased. The highest activity was observed for the sample containing only mononuclear Au(III) complexes. Cationic gold was observed by XANES along with zerovalent gold clusters in the working catalysts when the clusters were relatively small (but the data were not sensitive enough to detect them when the clusters were larger). The data imply that zerovalent gold clusters and particles are not catalytically active for ethylene hydrogenation.

In summary, all the data are consistent with the identification of cationic gold complexes as the catalytically active species. There is no evidence of catalytic activity of gold clusters for ethylene hydrogenation, consistent with conventional wisdom about the lack of activity of bulk, zerovalent gold [41].

5.4. Formation of ethylene-derived ligands on supported metal complexes, supported clusters, and metal surfaces

Only π-bonded ethylene and ethyl were observed on the supported gold complexes during ethylene hydrogenation catalysis under the conditions of our experiments. The intensity of the peak assigned to π-bonded ethylene on mononuclear gold remained approximately constant as P_{hydrogen} and the catalytic activity increased (Fig. 6). In contrast, the ethyl band intensities increased with increasing P_{hydrogen} and as the catalytic activity increased (Fig. 6). The results are consistent with the suggestion that ethyl ligands on the gold are reactive intermediates in the hydrogenation of ethylene and that π-bonded ethylene is a spectator or involved as an intermediate in virtually equilibrated steps.

This observation is consistent with mechanisms suggested for the hydrogenation of ethylene on small supported metal clusters (Ir_4/MgO and Ir_4/γ-Al_2O_3 [3]), when IR spectra were used to identify di-σ-bonded ethylene, π-bonded ethylene, ethylidyne, and ethyl on the clusters during catalysis. Ethyl, di-σ-bonded ethylene, and π-bonded

[2] Calculated from Au–Au coordination numbers (first- and second-shell), geometrical shapes, and on the basis of a proposed model.

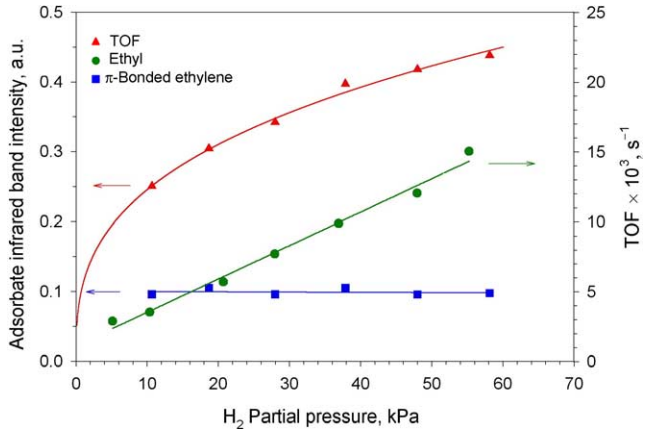

Fig. 6. Dependence of IR band intensities on H_2 partial pressure during ethylene hydrogenation catalyzed by mononuclear gold complexes supported on MgO. Catalytic activity (TOF, circles); the bands at 2960, 2923, and 2865 cm^{-1} were chosen to represent ethyl (triangles); and that at 3085 cm^{-1}, to represent π-bonded ethylene (squares).

ethylene were suggested to be reaction intermediates. Theoretical calculations for ethylene hydrogenation on the surface of Pd(111) show that di-σ-bonded ethylene and ethyl are reactive intermediates at low ethylene coverages [42]. Similarly, ethyl has been shown experimentally to be a reactive intermediate on the surface of Pt(111) [43,44].

Thus, we infer that ethylene hydrogenation catalysis on our sample is broadly similar to that catalyzed by the samples just described, with ethyl as a reactive intermediate. The lack of formation of di-σ-bonded ethylene may be associated with geometrical restrictions (the lack of metal atoms close enough together to allow formation of this ligand). A possible role of the support in the catalysis, such as in the adsorption of the H_2, cannot be ruled out.

6. Conclusions

XANES, EXAFS, and IR spectroscopies were used to investigate MgO-supported mononuclear gold complex catalysts during ethylene hydrogenation at 353 K. The results provide evidence of the stability of the metal complex, complex–support interactions, and reactant-derived ligands on the metal during ethylene hydrogenation catalysis. The EXAFS and XANES results demonstrate the stability of supported mononuclear Au(III) complexes during catalysis, and these complexes are identified as the catalytically active species. IR spectra demonstrate the presence of ethylene-derived ligands (adsorbates) on the gold during catalysis. Ethyl on the gold is suggested to be a reaction intermediate, with π-bonded ethylene being a spectator or involved in virtually equilibrated steps. Hydrogen on the gold is inferred from the order of the catalytic reaction in H_2 (0.5) to form by dissociative adsorption of H_2.

Acknowledgments

This research was supported by the U.S. Department of Energy, Office of Energy Research, Office of Basic Energy Sciences, Division of Chemical Sciences, Contract FG02-87ER13790. We acknowledge the National Synchrotron Light Source, Brookhaven National Laboratory, which is supported by the U.S. Department of Energy, Division of Materials Sciences and Division of Chemical Sciences, under Contract No. DE-AC02-98CH10886, and the staff of beamline X-11A.

References

[1] R.D. Cortright, S.A. Goddard, J.E. Rekoske, J.A. Dumesic, J. Catal. 127 (1991) 342.
[2] G.A. Somorjai, G. Rupprechter, J. Phys. Chem. B 103 (1999) 1623.
[3] A.M. Argo, J.F. Odzak, F.S. Lai, B.C. Gates, Nature 415 (2002) 623.
[4] B. Cornils, W.A. Herrmann, Applied Homogeneous Catalysis with Organometallic Compounds, second ed., 2002, VCH, Weinheim, 1996.
[5] J.F. Walzer Jr., U.S. patent 5643847 (1997).
[6] J. Guzman, B.C. Gates, J. Chem. Soc., Dalton Trans. 17 (2003) 3303.
[7] J.H. Teles, S. Brode, M. Chabanas, Angew. Chem. Int. Ed. 37 (1998) 1415.
[8] Y. Ito, M. Sawamura, T. Hayashi, J. Am. Chem. Soc. 108 (1986) 6405.
[9] A.S.K. Hashmi, L. Schwars, J.-H. Choi, T.M. Frost, Angew. Chem. Int. Ed. 39 (2000) 2285.
[10] F. Shi, Y. Deng, Chem. Commun. 5 (2001) 443.
[11] H. Ito, T. Yajima, J. Tateiwa, A. Hosomi, Chem. Commun. 11 (2000) 981.
[12] R. Casado, M. Contel, M. Laguna, P. Romero, S. Sanz, J. Am. Chem. Soc. 125 (2003) 11925.
[13] P. Landon, P.J. Collier, A.J. Papworth, C.J. Kiely, G.J. Hutchings, Chem. Commun. 18 (2002) 2058.
[14] S. Carrettin, P. McMorn, P. Johnston, K. Griffin, G.J. Hutchings, Chem. Commun. 7 (2002) 696.
[15] J.E. Bailie, G.J. Hutchings, Chem. Commun. 21 (1999) 2151; J.E. Bailie, H.A. Abdullah, J.A. Anderson, C.H. Rochester, N.V. Richardson, N. Hodge, J.-G. Zhang, A. Burrows, C.J. Kiely, G.J. Hutchings, Phys. Chem. Chem. Phys. 3 (2001) 4113.
[16] B. Nkosi, N.J. Coville, G.J. Hutchings, J. Chem. Soc., Chem. Commun. 1 (1988) 71.
[17] J. Guzman, B.C. Gates, Angew. Chem. Int. Ed. 42 (2003) 690.
[18] J.F. Odzak, A.M. Argo, F.S. Lai, B.C. Gates, K. Pandya, L. Feraria, Rev. Sci. Instrum. 72 (2001) 3943.
[19] M. Vaarkamp, J.C. Linders, D.C. Koningsberger, Phys. B 209 (1995) 159.
[20] M. Trömel, E.Z. Lupprich, Inorg. Chem. 414 (1975) 160.
[21] J. Guzman, Ph.D. dissertation, University of California, Davis, 2003.
[22] R.W.G. Wycoff (Ed.), in: Crystal Structures, second ed., vol. 1, Wiley, New York, 1963, p. 10.
[23] J.D.H. Donnay, H.M. Ondik, Crystal Data Determinative Tables, third ed., vol. II, U.S. Dept. of Commerce, National Bureau of Standards and the Joint Committee on Powder Diffraction Standards, USA, 1973, p. C-88.
[24] P.S. Kirlin, F.B.M. van Zon, D.C. Koningsberger, B.C. Gates, J. Phys. Chem. 94 (1990) 8439.
[25] J.B.A.D. van Zon, D.C. Koningsberger, H.F.J. van't Blik, D.E. Sayers, J. Chem. Phys. 82 (1985) 5742.
[26] S. Shibata, K. Iijima, T.H. Baum, J. Chem. Soc., Dalton Trans. 4 (1990) 1519.
[27] D.C. Koningsberger, B.C. Gates, Catal. Lett. 14 (1992) 271.

[28] J. Guzman, B.C. Gates, J. Phys. Chem. B 107 (2003) 2242.
[29] J. Guzman, B.C. Gates, J. Phys. Chem. B 106 (2002) 7659.
[30] R.E. Benfiled, D. Grandjean, M. Kröll, R. Pugin, T. Sawitowski, G. Schmid, J. Phys. Chem. B 105 (2001) 1961.
[31] T.M. Salama, T. Shido, R. Ohnishi, M. Ichikawa, J. Phys. Chem. 100 (1996) 3688.
[32] A.M. Argo, J.F. Odzak, B.C. Gates, J. Am. Chem. Soc. 125 (2003) 7107.
[33] A.M. Argo, B.C. Gates, J. Phys. Chem. B 107 (2003) 5519.
[34] B.E. Bent, C.M. Mate, C.-T. Kao, A.J. Slavin, G.A. Somorjai, J. Phys. Chem. 92 (1988) 2862.
[35] B.J. Bandy, M.A. Chesters, D.I. James, G.S. McDougall, M.E. Pemble, N. Sheppard, Philos. Trans. R. Soc. London Ser. A 318 (1986) 141.
[36] M.-J. Crawford, T.M. Klapötke, Angew. Chem. Int. Ed. 41 (2002) 2269.
[37] X. Wang, L. Andrews, J. Am. Chem. Soc. 123 (2001) 12899.
[38] T. Shimanouchi, Tables of Molecular Vibrational Frequencies, Natl. Stand. Ref. Data Ser. (US, Natl. Bur. Stand.) 1 (1962) 39.
[39] K.G. Lloyd, B. Roop, A. Campion, J.M. White, Surf. Sci. 214 (1989) 227.
[40] A. Jentys, Phys. Chem. Chem. Phys. 1 (1999) 4059.
[41] M. Haruta, M. Daté, Appl. Catal. A 222 (2001) 427.
[42] M. Neurock, R.A. van Santen, J. Phys. Chem. B 104 (2000) 11127.
[43] P.S. Cremer, X. Su, Y.R. Shen, G.A. Somorjai, Catal. Lett. 40 (1996) 143.
[44] P.S. Cremer, X. Su, Y.R. Shen, G.A. Somorjai, J. Am. Chem. Soc. 118 (1996) 2942.